A

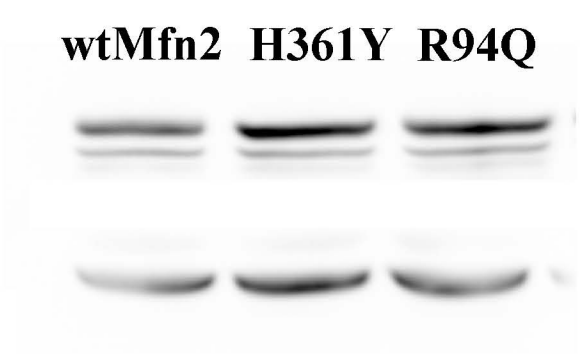
wtMfn2
H361Y
R94Q
anti HA
anti Beta tubulin

B

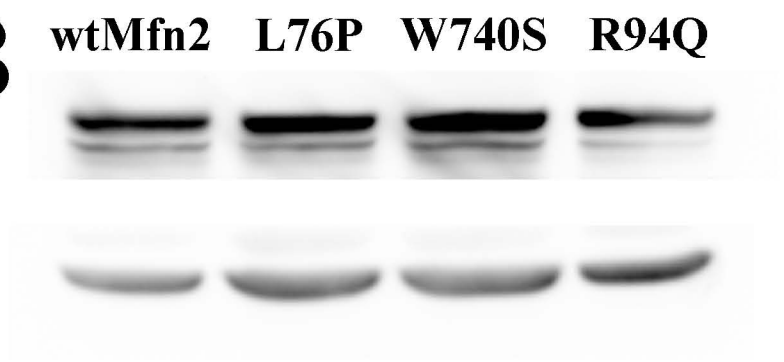
wtMfn2
L76P
W740S
R94Q
anti HA
anti Beta tubulin

C

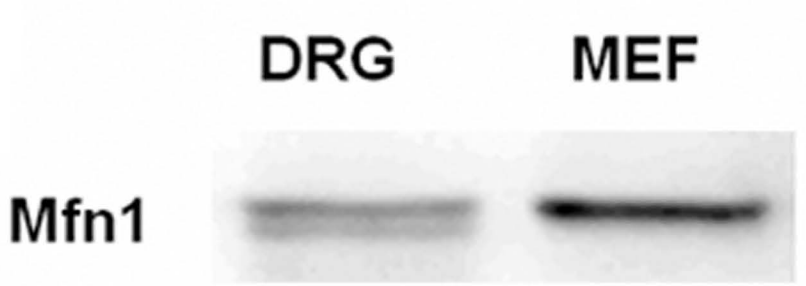
DRG
MEF
Mfn1

D

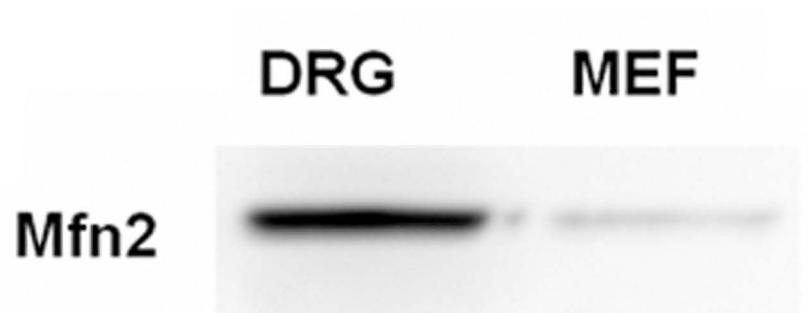
DRG
MEF
Mfn2

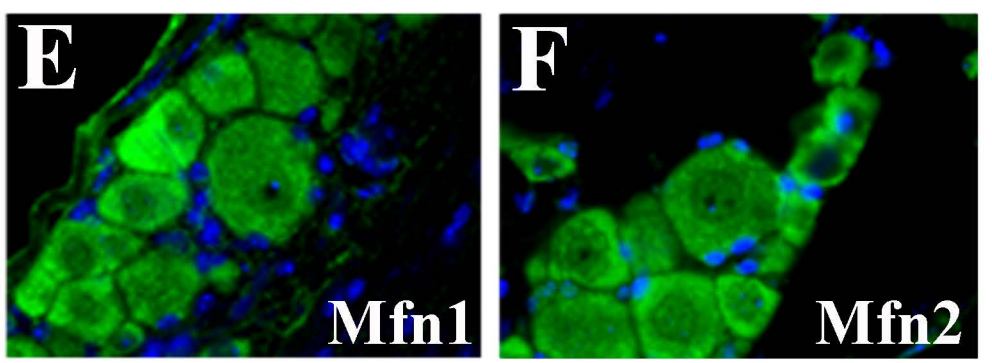
E
Mfn1
F
Mfn2

G

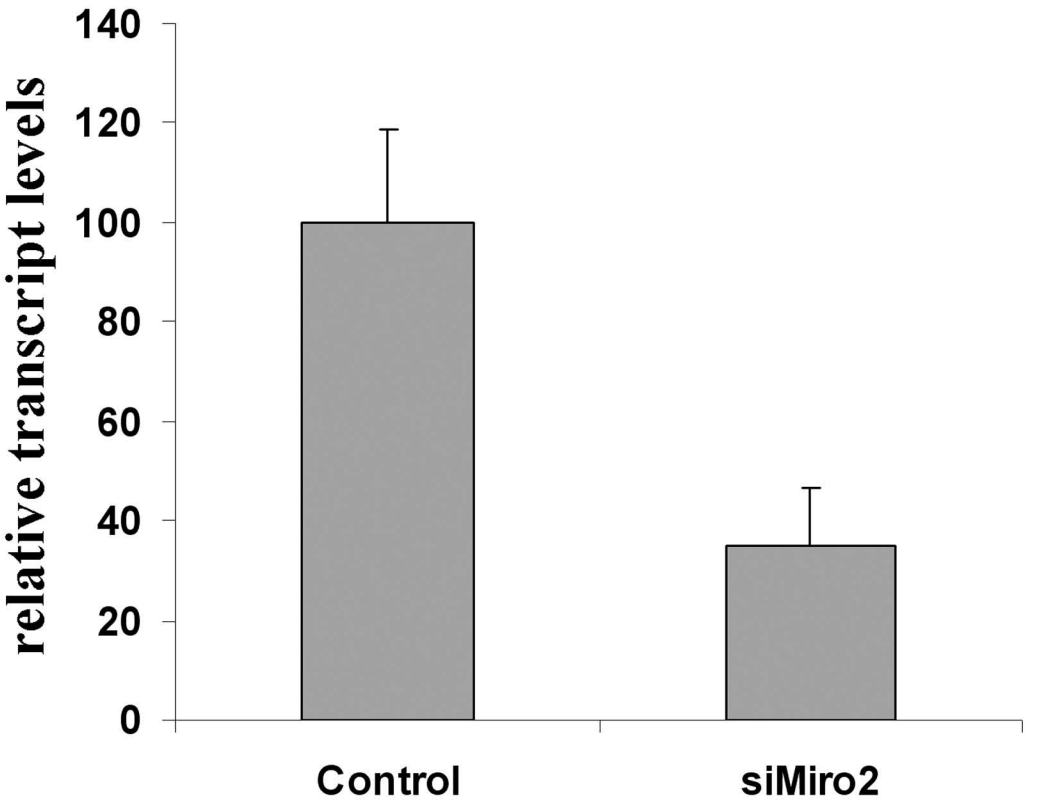
relative transcript levels
140
120
100
80
60
40
20
0
Control
siMiro2

H

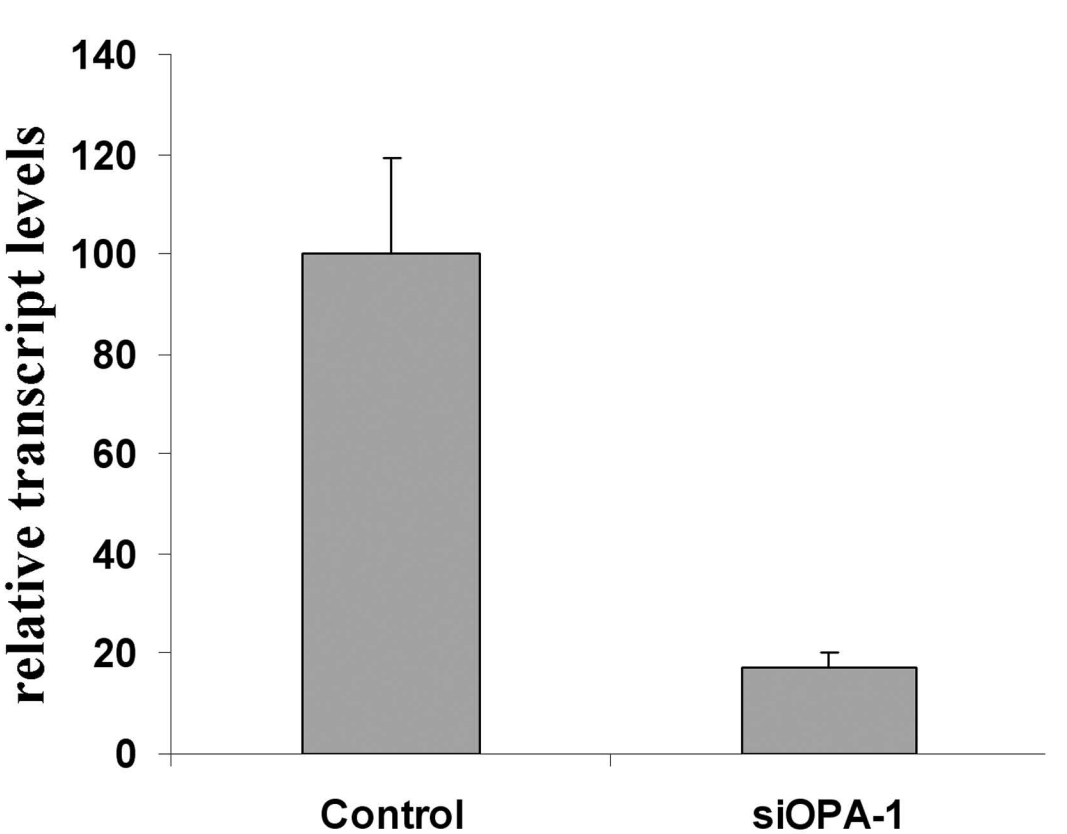
relative transcript levels
140
120
100
80
60
40
20
0
Control
siOPA-1

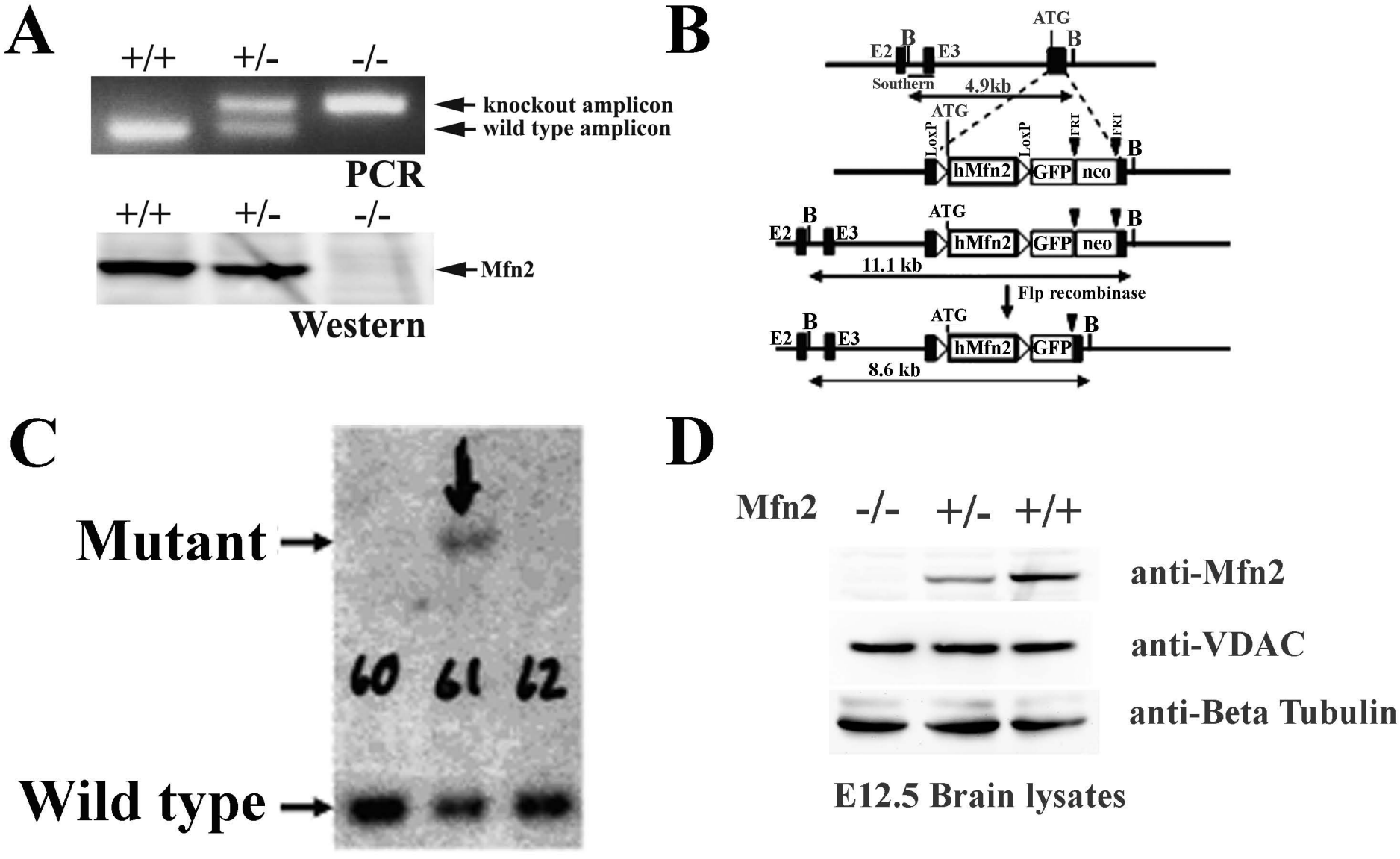
A
+/+
+/-
-/-
knockout amplicon
wild type amplicon
PCR
+/+
+/-
-/-
Mfn2
Western
B
ATG
B
E2
E3
B
Southern
4.9kb
ATG
LoxP
LoxP
FRT
FRT
B
hMfn2
GFP
neo
B
E2
E3
ATG
hMfn2
GFP
neo
B
11.1 kb
Flp recombinase
B
E2
E3
ATG
hMfn2
GFP
B
8.6 kb
C
Mutant
60
61
62
Wild type
D
Mfn2
-/-
+/-
+/+
anti-Mfn2
anti-VDAC
anti-Beta Tubulin
E12.5 Brain lysates

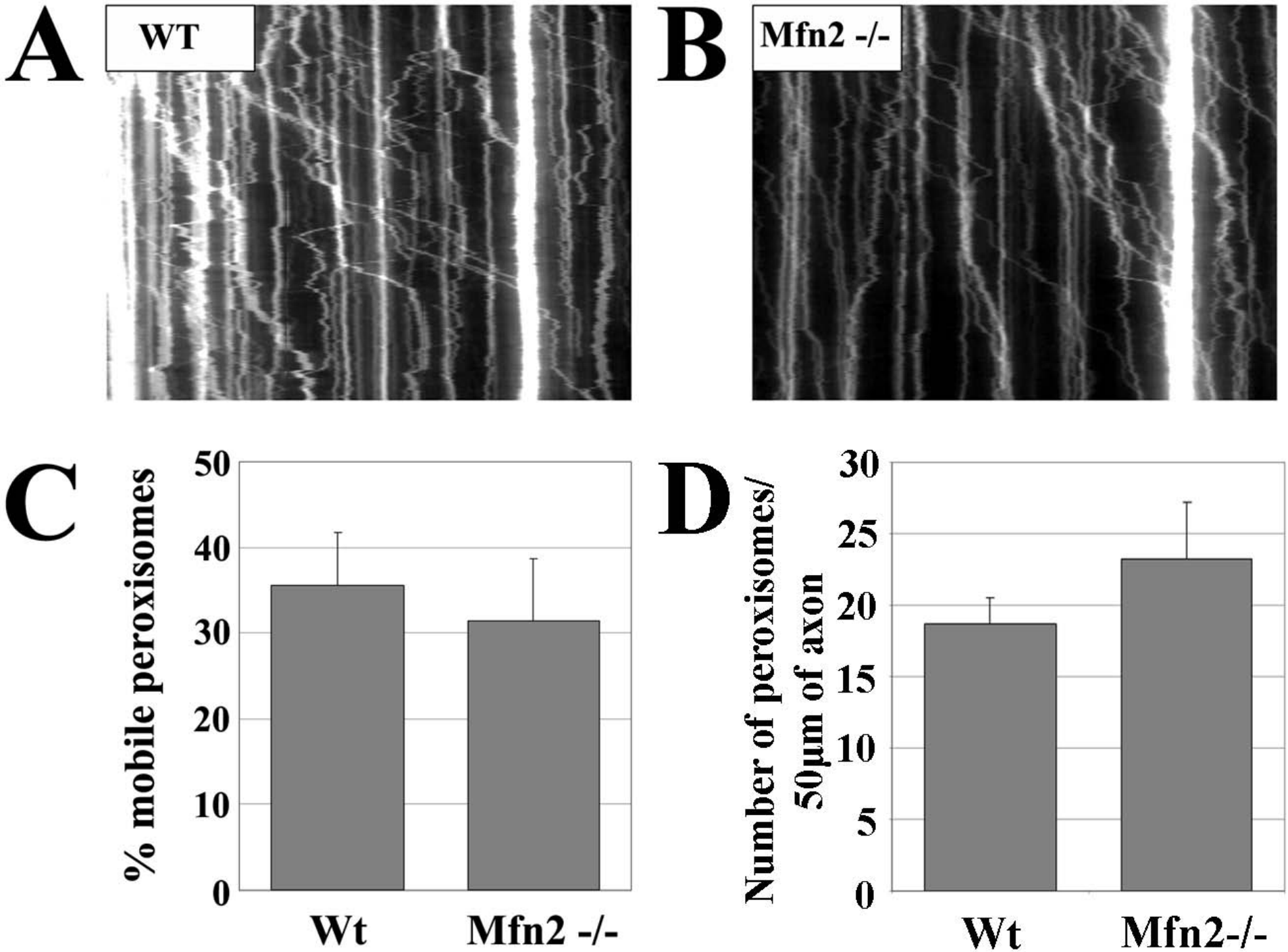
A
WT
B
Mfn2 -/-
C
% mobile peroxisomes
50
40
30
20
10
0
Wt
Mfn2 -/-
D
Number of peroxisomes/ 50µm of axon
30
25
20
15
10
5
0
Wt
Mfn2-/-

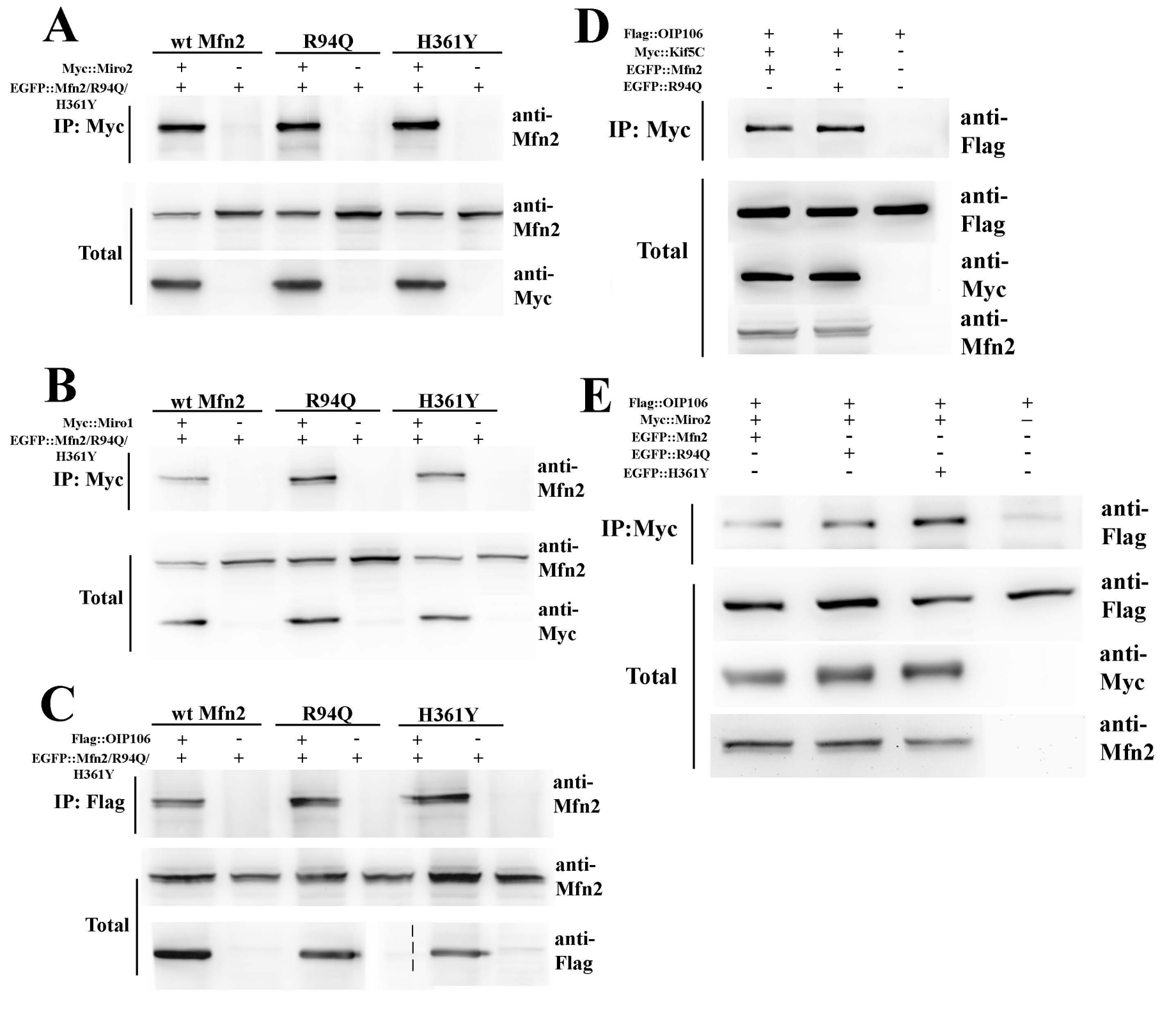
A
wt Mfn2
R94Q
H361Y
Myc::Miro2
EGFP::Mfn2/R94Q/
H361Y
IP: Myc
anti-
Mfn2
Total
anti-
Mfn2
anti-
Myc
B
wt Mfn2
R94Q
H361Y
Myc::Miro1
EGFP::Mfn2/R94Q/
H361Y
IP: Myc
anti-
Mfn2
Total
anti-
Mfn2
anti-
Myc
C
wt Mfn2
R94Q
H361Y
Flag::OIP106
EGFP::Mfn2/R94Q/
H361Y
IP: Flag
anti-
Mfn2
Total
anti-
Mfn2
anti-
Flag
D
Flag::OIP106
Myc::Kif5C
EGFP::Mfn2
EGFP::R94Q
IP: Myc
anti-
Flag
Total
anti-
Flag
anti-
Myc
anti-
Mfn2
E
Flag::OIP106
Myc::Miro2
EGFP::Mfn2
EGFP::R94Q
EGFP::H361Y
IP:Myc
anti-
Flag
Total
anti-
Flag
anti-
Myc
anti-
Mfn2

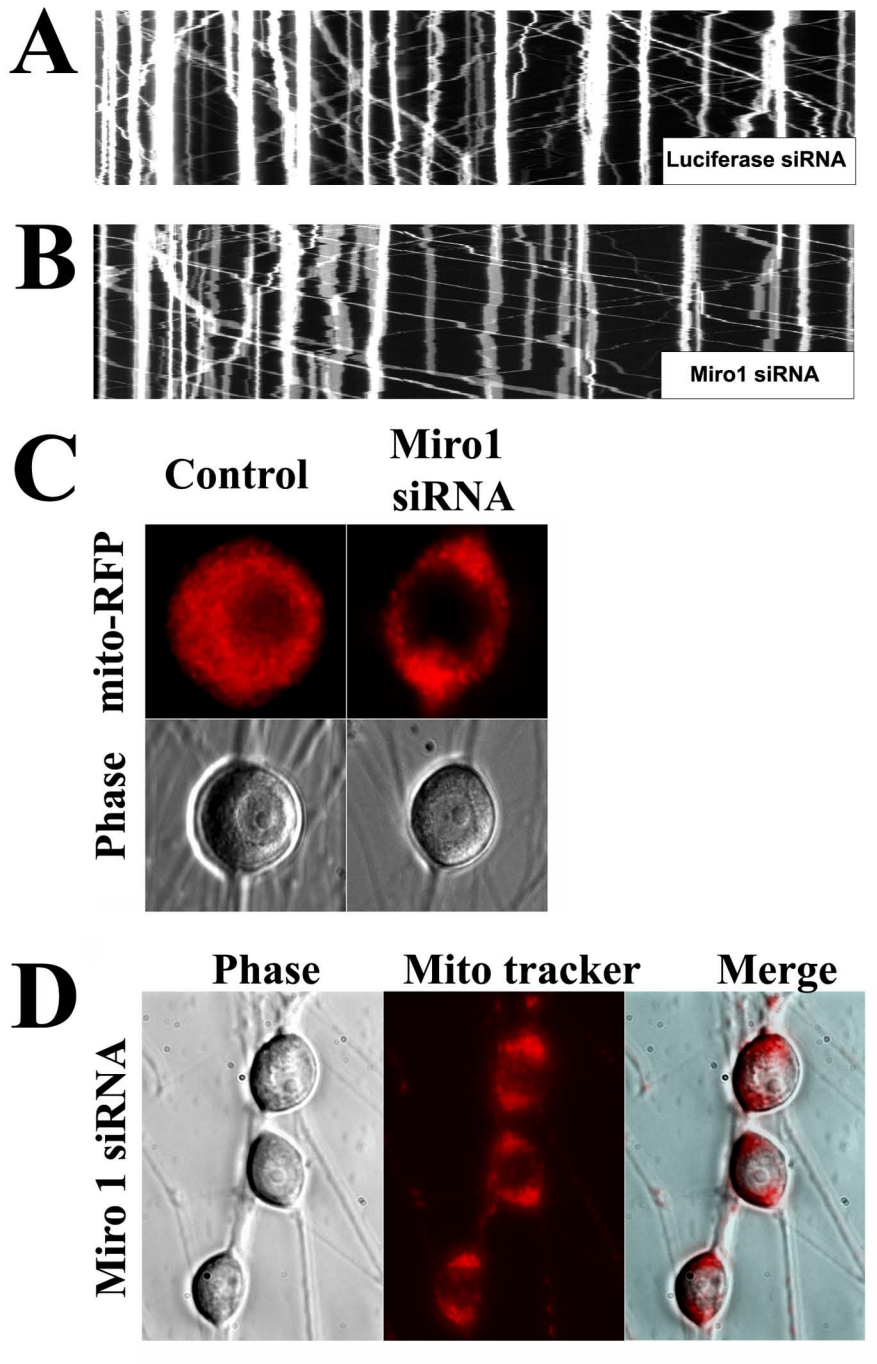
A
Luciferase siRNA
B
Miro1 siRNA
C
Control
Miro1 siRNA
mito-RFP
Phase
D
Phase
Mito tracker
Merge
Miro 1 siRNA

Supplementary Figure Legends

Figure S1. **Expression levels of MFN2 constructs in DRG neurons, western blot analysis of Mfn1 and Mfn2 in DRG and MEF cell lysates, and qPCR analysis of siRNA mediated knock down of Miro2 and OPA1 transcript levels in DRG neurons.** (A) Western blot analysis of virally transduced wtMfn2, R94Q and H361Y protein levels in rat DRG neuron cultures 7 days post infection, at the time when mitochondrial movements were analyzed, corresponding to constructs used in Figure 1. (B) Western blot analysis of wtMfn2, L76P, W740S and R94Q protein levels introduced by lentivirus infection into Mfn2-/- DRG neuron cultures. These viral constructs correspond to those in Figure 7. (C) Lysates were prepared from cultured wild type DRG neurons or MEF cells. Equal amounts of protein were separated by SDS PAGE and probed with antibodies against Mfn1. Relative amounts of Mfn1 protein were less in DRG neurons compared to MEF cells. Mfn1 appears as a doublet in DRG lysates whereas the lower molecular weight band is absent in MEF cells. (D) The same lysates were probed with antibody against endogenous Mfn2. Levels of Mfn2 are greater in DRGs compared to MEF cells. (E,F) Immunofluorescence labeling of paraffin embedded sections shows that Mfn1 and Mfn2 are both expressed in adult mouse DRG neurons. Quantitative PCR analysis demonstrated (G) ~70% knockdown of Miro2 and (H) ~90% knockdown of OPA1 transcript levels in rat DRG neuron cultures 7 days after infection with the siRNA construct, at the time when mitochondrial movements were measured.

Figure S2. **PCR and Western blot genotyping of Mfn2 knockout mouse line.**

(A) Primers were designed with a common genomic forward primer and reverse primers residing in either the wild type Mfn2 allele or the recombinant allele. Panel A depicts a wild type, heterozygous and homozygous mouse (from left to right). Although this was originally designed to knock in the human cDNA, western blot analysis on brain lysates from E12.5 embryos using an antibody against Mfn2 (or the HA tag on the cDNA) revealed the absence of protein in homozygous mice. This indicated that the knocked in cDNA was not expressed, and furthermore the insertion of the knock-in allele in the first coding exon completely suppressed expression of the endogenous mouse Mfn2 locus. (B) Schematic of targeting construct, initially designed to knock-in a mutant allele. The human MFN2 (hMFN2) cDNA with an SV40 intron and polyadenylation signal was inserted via homologous recombination into exon 4 (E4), the first coding exon. The neomycin resistance cassette is flanked by FRT sites, and was removed by breeding to mice expressing the Flp recombinase. (B – BamHI site). (C) Southern blot of BamHI digested ES cell DNA showing bands at the predicted size (wild-type 4.9 kb, recombined 11.1 kb) for both the wild-type and recombinant alleles at the MFN2 locus in clone 61. (D) Mitochondrial content is unchanged in Mfn2-/- mice. We performed western blot analysis on E12.5 brain lysates from wild type, heterozygous and homozygous littermates and used the OMM protein VDAC as a marker for mitochondrial content. While Mfn2 protein levels are absent or decreased in Mfn2 null (-/-) and Mfn2 heterozygotes (+/-) respectively, VDAC levels as a measure of total mitochondrial content remain unchanged.

Figure S3. **Peroxisomal movement and content are unchanged in axons of Mfn2-/- DRGs.** (A, B) Peroxisomes were labeled with a GFP-SKL fusion protein and introduced into DRG cultures by Lentiviral infection. Time lapse microscopy was used to examine peroxisome movements in wild type and Mfn2-/- neurons. Movements on kymograph analysis depicted on panels A and B show that peroxisomal transport appears normal in knockout cultures. (C) The percentage of mobile peroxisomes is not significantly different between wild-type and Mfn2-/- neurons. (D) Counts of number of peroxisomes per 50μm of axon show that peroxisomal content is not significantly different between Wt and Mfn2-/- cells.

Figure S4. **CMT2A associated MFN2 disease mutants maintain interactions with components of the mitochondrial transport apparatus and do not disrupt formation of the Miro/Milton/Kinesin complex.**

(A and B) Both Miro2 and Miro1 are able to coimmunoprecipitate with R94Q and H361Y as well as with wtMfn2. (C) OIP106 coimmunoprecipitates with R94Q and H361Y as well as with wtMfn2. (D) OIP106 maintains its ability to interact with Kif5C in the presence of R94Q. (E) Miro2 maintains its ability to interact with OIP106 in the presence of R94Q or H361Y.

Figure S5. **Miro1 knock down alters mitochondrial distribution in the cell bodies of DRG neurons but does not abolish axonal transport.**

(A,B) Kymograph analysis of mitochondrial transport in Miro1 knock down DRG neurons showed normal patterns of mitochondrial movements when compared to controls

infected with siRNA against luciferase. (C) DRG neurons coinfected with control or Miro1 siRNA virus and mito-RFP virus show altered distribution of mitochondria to clusters in polar regions of the cell body. (D) Mitotracker staining of Miro1 knock down DRG neurons also reveals altered distribution of mitochondria in cell bodies.